

International Journal of Nanomanufacturing

ISSN online: 1746-9406 - ISSN print: 1746-9392

<https://www.inderscience.com/ijnm>

Study on the effect of self-heating effect of bulk acoustic wave filter on the interpolation loss in the band

Bin Ruan, Tingting Liu, Shaohua Yang, Qinwen Huang, Ming Wu, Weiheng Shao

DOI: [10.1504/IJNM.2023.10060119](https://doi.org/10.1504/IJNM.2023.10060119)

Article History:

Received:	22 March 2023
Last revised:	23 March 2023
Accepted:	30 June 2023
Published online:	07 February 2024

Study on the effect of self-heating effect of bulk acoustic wave filter on the interpolation loss in the band

Bin Ruan and Tingting Liu

School of Information Engineering,
Southwest University of Science and Technology,
No. 59, Qinglong Road, Sichuan Province, Mianyang, 621010, China
Email: 2504096573@qq.com
Email: liutingting@swust.edu.cn

Shaohua Yang* and Qinwen Huang

Science and Technology on Reliability Physics and Application
Technology of Electronic Component Laboratory,
China Electronic Product Reliability, and Environmental Testing
Research Institute,
Guangdong Province, Guangzhou, 510610, China
Email: 2504096573@qq.com
Email: young01@163.com
Email: 971230012@163.com
*Corresponding author

Ming Wu

Pandhus Microsystem Co., Ltd.,
Room 301, Building 3, Innovation Centre Phase 2,
Science and Technology Business Park, Mianyang, Sichuan, China
Email: huajingkj@sina.com

Weiheng Shao

Science and Technology on Reliability Physics and Application
Technology of Electronic Component Laboratory,
China Electronic Product Reliability, and Environmental Testing
Research Institute,
Guangdong Province, Guangzhou, 510610, China
Email: shaoweiheng@126.com

Abstract: The self-heating effect occurs when the bulk acoustic wave filter is loaded with power, leading to the deterioration of the insertion loss. In this paper, the self-heating effect of bulk acoustic wave filters at high frequency power is investigated. A test system is built to obtain the maximum surface temperature and the insertion loss of the bulk acoustic wave filter at different power levels. The test results show that the self-heating effect causes the

internal temperature of the bulk acoustic wave filter to increase further after increasing the power, resulting in the increase of the insertion loss. The test system and analysis method in this paper verify the relationship between the self-heating effect and the insertion loss, and can provide guidance for the construction of the relevant reliability test system of the bulk acoustic wave filter.

Keywords: bulk acoustic wave filter; self-heating effect; insertion loss.

Reference to this paper should be made as follows: Ruan, B., Liu, T., Yang, S., Huang, Q., Wu, M. and Shao, W. (2023) 'Study on the effect of self-heating effect of bulk acoustic wave filter on the interpolation loss in the band', *Int. J. Nanomanufacturing*, Vol. 18, Nos. 3/4, pp.178–188.

Biographical notes: Bin Ruan is a Master's student in Electronic Information at Southwest University of Science and Technology. Jointly trained by Southwest University of Science and Technology and the China Electronic Produce Reliability and Environmental Testing Research Institute (CEPREI), he is mainly engaged in the reliability research of MEMS devices.

Tingting Liu is an Associate Professor, PhD, Master's Supervisor, Senior member of Chinese Society of Micro and Nanotechnology. He is mainly engaged in the research of microfluidic technology, MEMS devices and measurement and control systems, and has published more than 10 academic papers in recent years, including 2 SCI and 6 EI papers. At present, he is presiding over 1 project of National Natural Science Foundation of China, 1 key project of Sichuan Education Department, 2 projects of National Natural Science Foundation of China, 2 projects of National Defense Fundamental Research Project, 1 project of 863 Project, and many horizontal projects.

Shaohua Yang is a Senior Engineer at the Ministry of Industry and Information Technology, No. 5 Electronics Research Institute, Guangzhou, and is mainly engaged in the research of electronic component reliability. He has published 53 journal and conference papers, mainly in the field of physics.

Qinwen Huang received his BS and MS degrees in Applied Physics from the South China University of Technology, Guangzhou, China, in 2001 and 2004, respectively, and the PhD degree from the Institute of Microelectronics, Chinese Academy of Sciences, Beijing, China, in 2007. He is a senior engineer of the Ministry of Industry and Information Technology, No. 5 Electronics Research Institute, Guangzhou. His current research interests include the fields of experimental methods design for microelectromechanical system (MEMS) inertial sensors and MEMS reliability.

Ming Wu is the Legal Representative of Huajing Technology Co., Ltd. The company's business scope includes: computer software and hardware, electronic products, integrated circuits and communications equipment research and development, etc.

Weiheng Shao received his BE and ME degrees in Electrical Engineering from Northeastern University, ShenYang, China, in 2012 and 2014, respectively. Since 2021, he has been pursuing the PhD degree in Electronic Information Engineering at South China University of Technology, Guangzhou, China. Since 2014, he has been with China Electronic Produce Reliability and Environmental Testing Research Institute (CEPREI). His current interests include electromagnetic environment reliability in integrated circuits, component, and system level.

1 Introduction

Mobile 5G communication and smart devices are now in a high development stage and their intelligence requires radio communication for information interaction (Aigner and Fattinger, 2019). Therefore, highly reliable radio frequency (RF) devices are needed to send and receive information. Currently, the commonly used filters in RF are surface acoustic wave (SAW) filters and bulk acoustic waves (BAW) filters. SAW filters are limited to operate in the low to medium frequency band of kHz. In contrast, BAW filters can operate in the high frequency band with high power capacity, high energy conversion efficiency, high out-of-band rejection and low insertion loss (IL), so they are commonly used in RF front ends of various devices (Chen et al., 2021; Strijbos et al., 2007; Ruppel, 2017), such as magnetolectric transducer antennas for wireless communication (Chen et al., 2022). In addition, BAW filters can be applied in physical sensors and actuators as well as biochemical sensors (Yang et al., 2022). Thus, it is evident that BAW filters have excellent performance and a wide range of uses, and therefore it is necessary to pay more attention to their operating performance.

One important parameter of BAW filters is the *IL*, which reflects the loss generated by the power signal through the filter (Lakin, 1999). The smaller the *IL*, the better the transmission performance of the BAW filter, and vice versa. The internal temperature of the BAW filter increases at high power, which reduces the performance of the BAW filter (Aigner et al., 2005, Tag et al., 2014). The thermal behaviour of BAW filters at high power has been simulated by finite element and the temperature distribution and heat transfer path of the internal piezoelectric layer of BAW filters have been obtained (Kirkendall and Ivira, 2018, Kozlov, 2019). However, there is a lack of research on BAW filters under actual operating conditions. In this paper, we build a test system for BAW filters to study the maximum surface temperature and the variation of the *IL* of BAW filters at different powers.

2 BAW filter

The basic component unit of BAW filters is the BAW resonator, which is mainly divided into thin film bulk acoustic wave resonator (FBAR) and solidly mounted resonator (SMR) (Kozlov, 2021). Both of these resonators are widely used, but the reflection of acoustic waves by the Bragg reflection layer in SMR is not as good as the reflection of acoustic waves by the air in FBAR, so some of the acoustic waves will still leak out through the substrate, thus causing energy loss (Farina and Rozzi, 2004, Schaefer et al., 2019). Therefore, in this paper, the BAW filter with FBAR as the basic component unit is used as the research object.

When an AC voltage is applied to the top and bottom electrodes of the FBAR, an inverse piezoelectric effect occurs in the piezoelectric layer and the electrical signal is converted to an acoustic wave and a standing wave is formed in the piezoelectric layer. When the frequency of the electric signal coincides with the standing wave frequency, the FBAR can output the signal of that frequency. The above is the working principle of FBAR to generate resonant frequency.

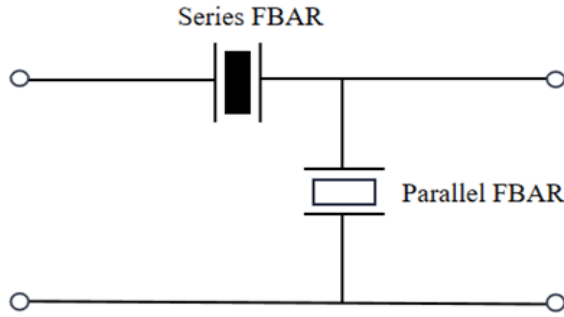
The FBAR exists at two resonant frequencies, the series resonant frequency f_s and the parallel resonant frequency f_p . From the FBAR impedance expression of equation (1), we

can obtain that the impedance of FBAR at f_s is zero and at f_p the impedance of FBAR is infinite (Jamneala et al., 2008).

$$Z = \frac{1}{j\omega C_0} \left[1 - k_t^2 \frac{\tan \phi_p}{\phi_p} \frac{(z_t + z_b) \cos^2 \phi_p + j \sin 2\phi_p}{(z_t + z_b) \cos 2\phi_p + j(z_t z_b + 1) \sin 2\phi_p} \right] \quad (1)$$

where ϕ is the imaginary part; ω is the angular frequency; C_0 is the static capacitance; k_t^2 is the electromechanical coupling coefficient of the piezoelectric layer; ϕ_p is the phase shift of the piezoelectric layer; Z_t is the acoustic impedance of the interface between the piezoelectric layer and the top electrode; Z_b is the acoustic impedance of the interface between the piezoelectric layer and the bottom electrode; Z_p is the characteristic acoustic impedance of the piezoelectric layer. Using the impedance characteristics of FBAR, multiple FBAR resonators are cascaded in series and parallel to form a trapezoidal structure, which constitutes a BAW bandpass filter. The topology of the first-order ladder BAW filter is shown in Figure 1.

Figure 1 First-order trapezoidal BAW filter topology



In the BAW filter topology, the resonant frequency of the parallel FBAR is smaller than that of the series FBAR. The series resonant frequency f_{ps} of the parallel FBAR is smaller than the series resonant frequency f_{ss} of the series FBAR. The impedance of the parallel FBAR at the frequency f_{ps} is extremely small, and the input signal is transmitted to ground through the parallel FBAR, and the BAW filter has no output signal. The parallel resonant frequency f_{pp} of the parallel FBAR is basically the same as f_{ss} , the impedance of the parallel resonator at this frequency is infinity, the impedance of the series resonator is zero, the signal is able to pass through the BAW filter with less loss, thus forming a passband. The impedance of the series FBAR at the parallel resonant frequency f_{sp} is extremely large, and the input signal cannot pass through the BAW filter. In summary, this is the filtering principle of the first-order trapezoidal BAW filter.

According to the operating principle of resonators and filters, it is known that the IL is related to the elasticity coefficient of the material, the longitudinal propagation speed of the acoustic wave, the resonant frequency and the quality factor. The following equation exists between the above parameters, and equation (2) is the formula for the elasticity coefficient:

$$C(T) = C(T_0) * C(T) = C(T_0) * [1 + TC(T - T_0)] \quad (2)$$

where $C(T)$ is the coefficient of elasticity at self-heating temperature, $C(T_0)$ is the coefficient of elasticity at room temperature, and TC is the temperature coefficient of the coefficient of elasticity.

Equation (3) is the calculation of the longitudinal propagation velocity of the acoustic wave in the material:

$$v = \sqrt{\frac{C + \frac{e^2}{\varepsilon}}{\rho}} \quad (3)$$

where v is the longitudinal propagation velocity of the acoustic wave in the piezoelectric layer, e is the piezoelectric stress constant, ε is the clamping dielectric constant, and ρ is the density of the piezoelectric layer material. Equation (4) is the resonant frequency of the resonator calculated as:

$$f = \frac{v}{2d} \quad (4)$$

where f is the resonant frequency and d is the thickness of the piezoelectric layer. Equation (5) is the formula for the quality factor,

$$Q = \frac{f}{2} \left| \frac{d\varphi}{df} \right| \quad (5)$$

where Q is the quality factor and φ is the impedance phase. The higher the Q value, the greater the IL and the better the passband transmission performance of the BAW filter.

3 Test system construction

3.1 System composition

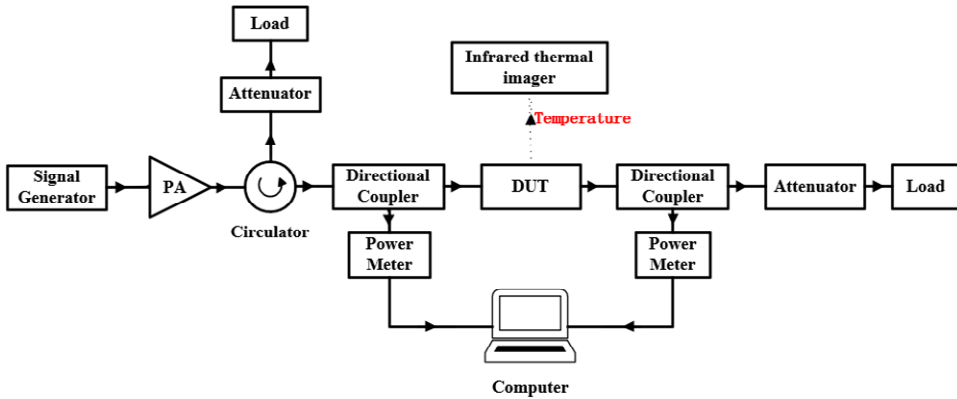
In order to observe the heating of the BAW filter at different input powers. The test system built needs to have the conditions to monitor both the maximum temperature of the BAW filter surface as well as the IL. Therefore the test environment is mainly divided into a power loading part and a measurement part. The power loading part consists of signal generator, power amplifier, circulator, directional coupler, attenuator and load; the measurement part consists of infrared thermal camera (model: TM-HST), power metre and computer. The built test environment is shown in Figure 2.

The power loading process of the test system is as follows: firstly, the power signal is generated by the signal generator; after that, it is transmitted to the power amplifier for amplification, and the amplified power signal is transmitted to the directional coupler by the circulator; then the power signal is loaded to the sample under test by the directional coupler; finally the power signal output from the sample under test is absorbed by the load after the directional coupler and attenuator.

During the power loading process, the *IL* and the maximum surface temperature of the sample under test are measured by the power metre and the infrared thermal imaging camera, respectively. The input and output power of the sample is measured by the power metre at both ends of the sample, and the absolute value of the difference between the two powers is the *IL*. The thermal imaging camera is able to measure the surface

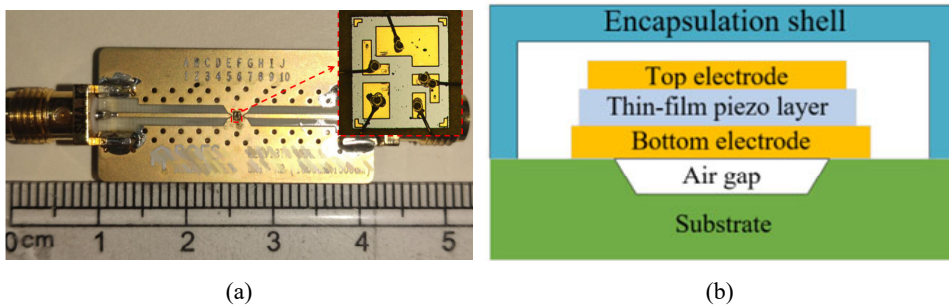
temperature distribution of the sample under test, and the maximum surface temperature of the sample under test can be obtained.

Figure 2 Test system construction (see online version for colours)



The purpose of testing other components of the system is to avoid damage to the system due to power signal injection failure. The reason for power signal injection failure is that when the frequency of the input power is in the resistance band, the signal will not pass through the filter and return along the path. The role of the circulator is to transmit the returned power signal to the attenuator to attenuate and then absorbed by the load to protect the power amplifier from damage. The role of the directional coupler is to transmit the power signal, and the equivalent signal attenuation 20 dB after input to the power metre to avoid damage to the power metre due to excessive power.

Figure 3 Diagram of the sample under test (a) fixture diagram and SEM image of the BAW filter (b) schematic diagram of the structure of the internal FBAR of the BAW filter (see online version for colours)



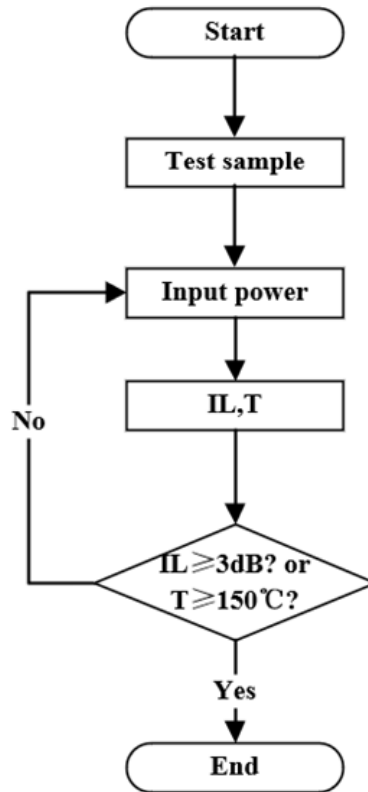
The sample under test is a BAW filter composed of an FBAR, which has two types of structures, an air-gap type and a silicon surface etched type (Yang et al., 2023). The FBAR used in the test is an air-gap type with an 'air-gap' and 'sandwich' structure. Two metal electrodes are sandwiched by a piezoelectric film to form a sandwich, and a vacuum chamber is constructed under the sandwich. The upper and lower electrodes of the interlayer are made of molybdenum (Mo), the piezoelectric material is aluminium nitride (AlN), and the material of the encapsulated housing is ceramic. The vacuum

chamber below the sandwich is obtained by etching the silicon substrate. Figure 3 shows the fixture diagram, scanning electron microscope (SEM) diagram and structure diagram of the BAW filter.

3.2 Testing process

According to the operating environment of BAW filter and referring to IEC 63155, the accelerated degradation test flow of step power is developed as shown in Figure 4. The input power is increased from 0.5 W in steps of 0.1 W. Each power is held for 5 minutes until the test is terminated when the *IL* exceeds 3 dB or the maximum surface temperature *T* exceeds 150 °C. It is worth noting that the surface maximum temperature and the *IL* need to be stabilised after each power change before recording the data.

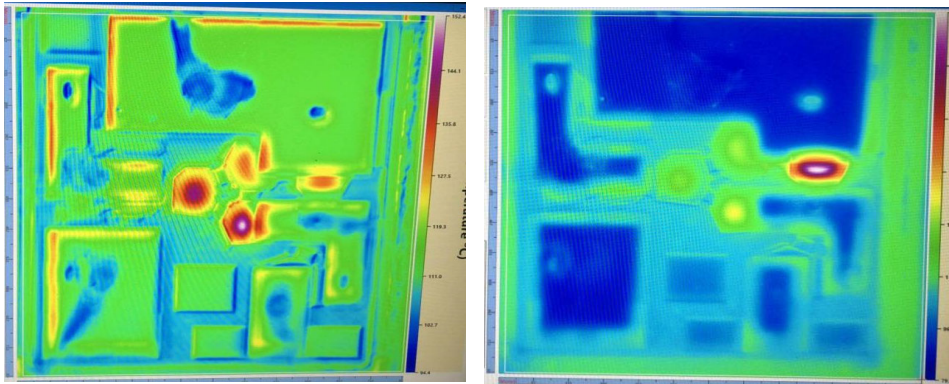
Figure 4 Test flow chart



3.3 Test results and analysis

The maximum surface temperature and the *IL* of the four samples at different powers, as well as the power limit of each sample, were obtained according to 3.2. The temperature distribution of the BAW filter surface shown in Figure 5 can be obtained by the infrared thermal imaging camera.

Figure 5 Surface temperature distribution of (a) the non-failed sample and (b) the failed sample (see online version for colours)



The temperature distribution graph before and after the BAW filter failure illustrates the significant reduction of heat concentration zones on the surface of the failed sample. The surface of the BAW filter before failure produces several high heat concentration areas, with the highest temperature area in the middle of the chip. Only a small area of the failed BAW filter shows a temperature increase at the same power input. The BAW filter heats up in the operating condition mainly because of the acoustic and electrical losses in the FBAR, while the temperature distribution plot of the failed sample shown in Figure 5(b) indicates that the sample has irreversible structural damage. The internal structure of this sample is damaged, which causes the series and parallel resonators inside the filter to be unable to receive power signals, and the piezoelectric layer and top and bottom electrodes do not pass through the power, so the heat generation area is reduced. The highest surface temperature of the failed sample is the power signal input region.

Figure 6 Test results (a) T-P and (b) IL-P (see online version for colours)

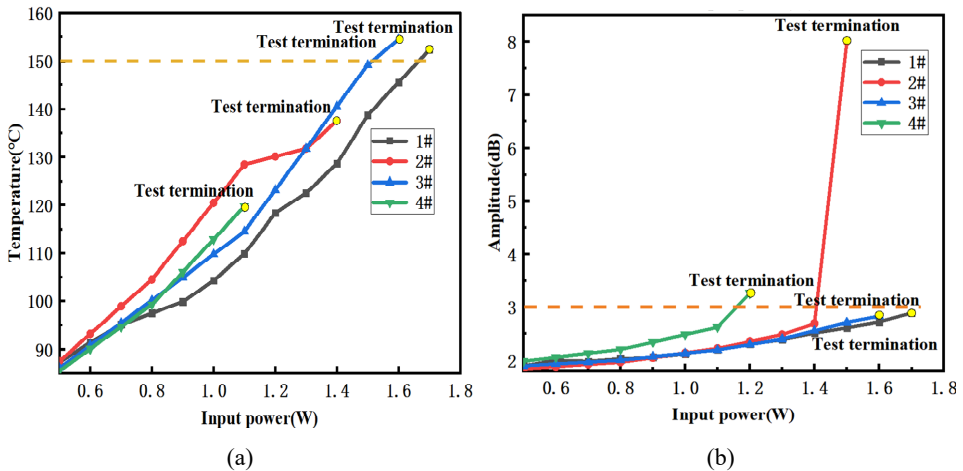


Figure 6 shows the maximum surface temperature and the *IL* measured at each stage of power, reflecting the trend of increasing BAW filter *T* and *IL* with increasing power. The

yellow dots in Figure 6 indicate that the samples reached T of 150 °C or IL greater than 3 dB at that power, so the four samples terminated the test at different power points. The test results show that the power limit of 1# is 1.7 W, the maximum temperature at this power is 152.3 °C, and the IL increases by 1 dB; the power limit of 2# is 1.5 W, the maximum at this power is 149.9 °C, and the IL increases by 6.17 dB; the power limit of 3# is 1.6 W, the maximum temperature at this power is 154.4 °C, and the IL increases by 0.94 dB; the power limit of 4# is 1.2 W, the maximum temperature at this power is 128.2 °C, and the IL increases by 1.28 dB. The more abnormal part of the red curve in Figure 6(b) reflects the failure of sample 2# with the IL greater than 3 dB when the input power increases from 1.4 W to 1.5 W.

Equation (6) enables to obtain the average input power rating of the BAW filter:

$$P_{in_aver} = \frac{1}{n} \sum_{i=1}^n P_i - 3 \quad (6)$$

where P_i is the input power corresponding to 1 dB of IL deterioration. The units of the power signal are converted from W to dBm for calculation, and the resulting calculation results are shown in Table 1.

The results show that the rated input power of the BAW filter is 0.733 W. The underlying reason for the increase in the IL of the BAW filter with increasing temperature is the decrease in the propagation speed of the acoustic wave in the piezoelectric material due to high temperature. After the input power is loaded into the BAW filter, it passes through the top electrode, piezoelectric layer and bottom electrode of the series and parallel FBAR. There are ohmic and wiring losses of the electrodes, attenuation losses of the acoustic wave and dielectric losses of the piezoelectric layer in the transmission path. The increase in power increases the losses through the FBAR and raises the temperature. The temperature increase reduces the elasticity coefficient of the AlN layer of the FBAR, which decreases the longitudinal propagation speed of the acoustic wave in the AlN layer, causing the resonant frequency to become smaller, resulting in a decrease in Q value, and eventually leading to the deterioration of the IL .

Table 1 Average power rating of the tested samples

<i>Sample</i>	<i>Insertion loss deterioration IdB input power(W)</i>	<i>Average rated input power (W)</i>
1#	1.7	0.733
2#	1.4	
3#	1.6	
4#	1.2	

4 Conclusions

This paper presents a method for simultaneous measurement of surface temperature and IL of a bulk acoustic wave filter. The theory that the IL of the bulk acoustic wave filter deteriorates with increasing temperature is verified by building a power loading part and a measurement part to form a test system and performing a power acceleration test with a step size of 0.1 W. The test results show that the power rating of the BAW filter is 0.733

W and the self-heating effect limits the power limit of the BAW filter. Each 0.1 W increase in input power causes a further increase in the maximum surface temperature and an increase in the IL. This study can be used as a guide for building test systems for other reliability studies of body acoustic wave filters, and has some reference value for improving the power rating of body acoustic wave filters.

Acknowledgements

The authors gratefully acknowledge the financial supports by the National Key R&D Program of China under grant number (2020YFB2008900), and the Key Research and Development Program of Guangzhou under Grant (202103020002).

References

- Aigner, R. and Fattinger, G. (2019) '3G–4G–5G: How BAW filter technology enables a connected world', in *2019 20th International Conference on Solid-State Sensors, Actuators and Microsystems and Eurosensors XXXIII (TRANSDUCERS and EUROSENSORS XXXIII)*, pp.523–526.
- Aigner, R., Huynh, N.H., Handtmann, M. and Marksteiner, S. (2005) 'Behavior of BAW devices at high power levels', in *IEEE MTT-S International Microwave Symposium Digest*, pp.429–432.
- Chen, S., Li, J., Gao, Y., Li, J., Dong, H., Gu, Z. and Ren, W. (2022) 'A micromechanical transmitter with only one BAW magneto-electric antenna', *Micromachines*, Vol. 13, No. 2, p.272.
- Chen, S., Ren, W.C., Li, J., Peng, C.R. and Gao, Y. (2021) 'Modeling of magnetic sensor based on BAW magneto-electric coupling micro-heterostructure', in *2021 IEEE 16th International Conference on Nano/Micro Engineered and Molecular Systems (NEMS)*, pp.1259–1263.
- Farina, M. and Rozzi, T. (2004) 'Electromagnetic modeling of thin-film bulk acoustic resonators', *IEEE Transactions on Microwave Theory and Techniques*, Vol. 52, No. 11, pp.2496–2502.
- International Electrotechnical Commission (2020) *IEC 63155:2020: Guidelines for the Measurement Method of Power Durability for Surface Acoustic Wave (SAW) and Bulk Acoustic Wave (BAW) Devices in Radio Frequency (RF) Applications*, Geneva, IEC.
- Jamneala, T., Bradley, P., Koelle, U.B. and Chien, A. (2008) 'Modified Mason model for bulk acoustic wave resonators', *IEEE Transactions on Ultrasonics, Ferroelectrics, and Frequency Control*, Vol. 55, No. 9, pp.2025–2029.
- Kirkendall, C. and Ivira, B. (2018) 'A hybrid 3D thermal/1D piezoelectric finite element model for rapid simulation of FBAR filter response under high power', in *2018 IEEE International Ultrasonics Symposium (IUS)*, pp.1–6.
- Kozlov, A.G. (2021) 'Effect of Bragg acoustic reflector on thermal processes in SMR under high power levels', in *2021 22nd International Conference on Thermal, Mechanical and Multi-Physics Simulation and Experiments in Microelectronics and Microsystems (EuroSimE)*, pp.1–6.
- Kozlov, A.G. (2019) 'Modeling of thermal processes in thin-film BAW resonators', in *2019 20th International Conference on Thermal, Mechanical and Multi-Physics Simulation and Experiments in Microelectronics and Microsystems (EuroSimE)*, pp.1–8.
- Lakin, K.M. (1999) 'Thin film resonators and filters', in *1999 IEEE Ultrasonics Symposium. Proceedings, International Symposium, 1999*, Vol. 2, pp.895–906.
- Ruppel, C.C. (2017) 'Acoustic wave filter technology—a review', *IEEE Transactions on Ultrasonics, Ferroelectrics, and FREQUENCY Control*, Vol. 64, No. 9, pp.1390–1400.

- Schaefer, M., Rothemund, R. and Fattinger, G. (2019) 'Process and design challenge for SMR-type bulk acoustic wave (BAW) filters at frequencies above 5 GHz', in *2019 IEEE International Ultrasonics Symposium (IUS)*, pp.1696–1699.
- Strijbos, R., Jansman, A., Lobeek, J.W., Li, N.X. and Pulsford, N. (2007) 'Design and characterisation of high-Q solidly-mounted bulk acoustic wave filters', in *2007 Proceedings 57th Electronic Components and Technology Conference*, pp.169–174.
- Tag, A., Weigel, R., Hagelauer, A., Bader, B., Huck, C., Pitschi, M. and Karolewski, D. (2014) 'Influence of dissipated power distribution on BAW resonators' behavior', in *2014 IEEE International Ultrasonics Symposium*, pp.2627–2630.
- Yang, Q., Xu, Y., Wu, Y., Wang, W. and Lai, Z. (2023) 'A 3.4–3.6 GHz high-selectivity filter chip based on film bulk acoustic resonator technology', *Electronics*, Vol. 12, No. 4, p.1056.
- Yang, Y., Dejous, C. and Hallil, H. (2022) 'Trends and applications of surface and bulk acoustic wave devices: a review', *Micromachines*, Vol. 14, No. 1, p.43.